J. Fluid Mech. (1974), *vol.* 62, *part* 1, *pp.* 185–207
Printed in Great Britain

The transverse force on a drop in an unbounded parabolic flow

By PHILIP R. WOHL
Department of Mathematics, New York University†
AND S. I. RUBINOW
Graduate School of Medical Sciences, Cornell University, New York

(Received 27 September 1972 and in revised form 16 July 1973)

The steady flow in and around a deformable liquid sphere moving in an unbounded viscous parabolic flow and subject to an external body force is calculated for small values of the ratio of the Weber number to the Reynolds number in the creeping-flow regime. It is found that, in addition to the drag force, the drop experiences a force orthogonal to the undisturbed flow direction. When the body force is absent (neutrally buoyant drop), this lift force tends to drive the drop inwards to the axis, where the undisturbed flow velocity is maximum, i.e., towards a position of lower velocity gradient. In the case for which the parabolic flow profile is a Poiseuille flow profile, the lift force is given by the expression

$$\mathbf{F}_1 = -6\pi\mu\epsilon U_0 \frac{\alpha+\frac{2}{3}}{\alpha+1}\left(\frac{a}{R_0}\right)^4 \mathbf{b}F[1+o(\epsilon)].$$

Here a is the radius of the undeformed sphere, R_0 is the radial distance from the position of maximum undisturbed flow U_0 at the profile axis to the position of zero flow, ϵ is the ratio of the Weber number to the Reynolds number, given by $\epsilon = \mu U_0 T^{-1}$, where μ is the external fluid viscosity and T is the surface tension of the drop, α is the ratio of the drop and external fluid viscosities, $\mathbf{b}$ is the radial vector from the flow axis to the centre of mass of the drop, and F is a function of α and a dimensionless parameter dependent on the body force that is determined in the analysis. Reasonable agreement is found between the observations by Goldsmith & Mason (1962) of the axial drift of liquid drops in Poiseuille flow and the predictions of the theory herein.

1. Introduction

We show that a deformable liquid sphere moving in an unbounded steady parabolic flow experiences a force orthogonal to its direction of motion, i.e. a life force, arising out of the interaction between the incident flow and the sphere deformation. Since we calculate the lift without taking into account inertial effects, our results are presumed to be valid for creeping flow. Our theoretical results are compared with the observations of Goldsmith & Mason (1962) on the radial migration of deforming drops in fluid flow in right circular cylindrical tubes, e.g. Poiseuille flow.

† Present address: Department of Mathematics, Carleton University, Ottawa, Ontario.

Motivation for the present study arose from the observations of axial accumulation of red blood cells in blood flowing through small arteries in the circulatory system. Evidence for this is the absence of red cells from a small region near the arterial wall, the so-called plasmatic zone. This effect is generally believed to be associated with a dynamical change in concentration of the red blood cells due to radial migration. The belief that red-cell migration is a purely hydromechanical effect is based in part on understanding of the dynamics of a rigid sphere in tube flow, and is the principal reason for likening a red cell to such a particle (Rubinow 1964). The effect of a decrease in apparent blood viscosity with an increase in bulk flow rate has been correlated with the degree of migration of particles in tube flow (Segre & Silberberg 1963). Moreover, the fact that a red blood cell is highly deformable *in vivo* (see Whitmore 1968) and has a viscous interior (Fung 1966) suggests that the dynamics of a deformable liquid sphere may provide better insight into the behaviour of a red cell.

The radial migration of a single spherical particle across the streamlines of a Poiseuille flow in a tube cannot be explained on the basis of Stokes' equations, even in the presence of the bounding walls; i.e. a sphere experiences no transverse force at zero Reynolds number. A transverse force does exist theoretically if inertial forces are taken into account (Rubinow & Keller 1961; Bjorklund 1965; Saffman 1965; Cox & Brenner 1968). However, the situation is different for flexible particles. The experimental observations of Goldsmith & Mason (1962), Karnis, Goldsmith & Mason (1963) and Karnis & Mason (1967) reveal that at low Reynolds numbers, even when a rigid sphere experiences a negligible transverse force, neutrally buoyant deforming drops (and flexible solid particles) migrate rapidly to the tube axis. It is reasonable to suppose, therefore, that the radial force producing axial migration of the deforming drops arises from the interaction between the drop deformation and the flow field around the drop, rather than from an inertial effect. Therefore, the force should be computable solely on the basis of the Stokes equations.

Chaffey, Brenner & Mason (1965, 1967) considered the problem of a deformable liquid sphere in Couette–Stokes flow. Assuming the drop to be 'close' to the plane wall bounding the flow, they found that the effect on the deformed drop was to produce a force tending to push the drop away from the wall. This force has two failings when used alone as a basis for explaining the inward migration of drops in Poiseuille flow. First, it neglects the force due to the interaction of the parabolic flow with the resultant deformation of the drop calculated herein. Second, it cannot be expected to be valid when the drop is not close to the wall. In fact, Karnis & Mason (1967) have shown experimentally that the migration rates calculated by Chaffey *et al.* are significantly larger than those which are observed. The experimental observations were recorded at a considerable distance from the tube walls relative to the particle size. For such observations, one might expect the effect of the unbounded parabolic flow profile to be more important than any perturbations introduced into the flow by proper consideration of the effect of the walls.

It is the purpose of this work to calculate the hydrodynamic viscous transverse force experienced by a deformable liquid sphere in an unbounded parabolic flow,

subject to an external body force. Our results are obtained by solving the Stokes equations for the motion of the liquids inside and outside the drop. In § 2, the problem is formulated in general. In § 3, a small perturbation procedure (see also Cox 1969) is presented which specifies the boundary conditions for the slightly perturbed sphere surface in terms of known fields on the undeformed sphere surface. This method is then used in § 4 to compute the flow in and around a drop in a parabolic profile by making use of the known solutions for spherical drops in steady uniform streams, linear shear flows and quadratic shear flows, respectively.

The resultant lift on the drop is calculated in § 5. Our result for the lift force is in significant quantitative disagreement with a similar calculation of the lift force performed by Haber & Hetsroni (1971). The small perturbation expansions used by us explicitly and by Haber & Hetsroni implicitly are apparently the same, to order ϵ. The deformation of the drop which is a consequence of the zero-order flow solution is also the same in both calculations.

The essential difference in procedure appears to be in the application of the 'natural' boundary conditions, equations (2.3) and (2.4), which must be applied at the surface of the deformed drop. Assuming the deformation of the drop to be small, these conditions are applied by us directly to the perturbed first-order flow and pressure fields. We relate the natural co-ordinate system fixed to the drop surface, through a small rotation, to a spherical co-ordinate system whose origin is fixed at the centroid of the drop. This small rotation is defined with the aid of two Eulerian angles, which are expressed in terms of the deformation of the drop.

By contrast, Haber & Hetsroni did not find it convenient to deal with the boundary conditions directly, but instead used a presumably equivalent set of boundary conditions. In place of continuity of the tangential velocity and stress, they required continuity of the velocity and stress acted on by various vector operators. One consequence of this difference is that our expressions for the boundary conditions on the order-ϵ flow field in terms of the vector components of the flow field cannot be compared with any corresponding expressions in their work. We are in fact only able to compare the final resulting lift force.

The validity and interpretation of the results for very viscous drops are discussed (§ 6). Some new results concerning the flow past rigid bodies are deduced. The small deformation of a very viscous drop on which tensile forces can be neglected was first investigated by Taylor (1934) in the case of an incident linear shear flow. His result for the deformation is different from the deformation calculated here, which is based on the assumption that interfacial tensile forces are large compared with viscous forces. This difference has undoubtedly contributed to the misapprehension that it is never permissible to let the viscosity of the fluid inside the drop *approach infinity*, when using such a small perturbation expansion.

The resultant trajectory of the drop is obtained (§ 7), and comparison is made (§ 8) with the observations of Goldsmith & Mason (1962) of neutrally buoyant liquid drops in a Poiseuille flow in a tube. The justification for comparing our theoretical results for the force in an unbounded parabolic flow with that in flow in a tube is based on the following considerations. It may be expected that the

forces on deformable particles in unbounded parabolic flow which coincides with a Poiseuille flow profile in the region of positive flow are a good approximation to the forces on such particles in actual tube flow when the particles are far from the wall, so that the 'wall effect' is negligible. By 'wall effect', we mean the secondary effect of the wall on the perturbed flow produced by the drop, and not the initial effect of the wall in producing the Poiseuille flow in the absence of the drop. Thus, it is expected that the theory is valid when the distance of the drop from the wall is large compared with the 'size' of the drop. A necessary condition for this criterion is that the tube radius is large compared with the radius of the drop.

Haber & Hetsroni also calculated the trajectories for a drop in Poiseuille flow, on the basis of their derived force. They predicted that a neutrally buoyant drop would move radially outwards whereas such drops are seen to move radially inwards, in agreement with our results. These authors made an algebraic error in sign in deriving their trajectories, which invalidates their results. If this error were corrected, their theory would also predict an inward migration, but the magnitude would remain in serious quantitative disagreement with observation. The trajectories predicted by the present theory for neutrally buoyant drops are in good agreement with the observations of Goldsmith & Mason (1962). This agreement lends support to our theoretical results.

2. Formulation

We wish to consider the steady motion of a drop of viscous fluid suspended in another viscous fluid which possesses a steady velocity distribution $\mathbf{U}$ far from the drop. $\mathbf{U}$ is measured relative to a spherical co-ordinate system with its origin fixed at the centroid of the drop, with the positive-z axis pointing in the direction of $\mathbf{U}$. In §4, we specialize $\mathbf{U}$ to be a parabolic flow, for example, a Poiseuille flow in a tube (see figure 1). It is assumed that there is a body force $\mathbf{K}_0$ per unit volume acting on the drop in the positive-z direction. In its quiescent state, the drop is spherical in shape and is maintained that way because of surface tension. The motion of the fluids causes in general a deformation of the drop away from its undisturbed, spherical shape. We shall assume that the fluid outside the drop is Newtonian, incompressible and viscous with viscosity μ.

We denote the velocity of the exterior fluid by $\mathbf{v}$ and the pressure by p. All external lengths, velocities and stresses have been non-dimensionalized by a, U_0 and $\mu U_0 a^{-1}$, respectively, where a is the radius of the undeformed spherical drop and U_0 is a reference velocity to be specified later. The same quantities when referring to the interior of the fluid drop are designated with a prime. The equation of the surface of the drop in the deformed state is represented by

$$r = 1 + f(\theta, \Phi), \tag{2.1}$$

where θ and Φ are angular co-ordinates of the spherical co-ordinate system. We shall assume that the fluids are immiscible, surface-active agents are absent and the (dimensional) surface tension T is constant. It is assumed that the flow is

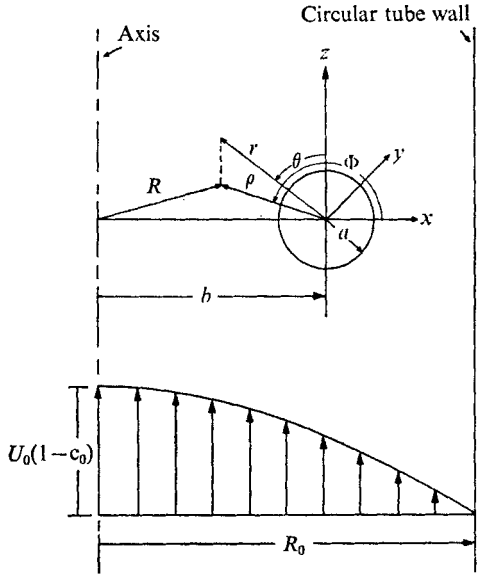

FIGURE 1. Geometry of Poiseuille flow incident on spherical drop located a distance b from position of tube axis. The fixed co-ordinate system has its origin at the centroid of the drop. With respect to this co-ordinate system, the flow field at infinity is given by (4.2a). Note that Φ is the angle in the x, y plane between the x axis and the vector $\boldsymbol{\rho}$ which is the projection of $\mathbf{r}$ on the x, y plane.

slow and that inertial effects are negligible, so that $\{\mathbf{v},\}p$ and $\{\mathbf{v}',p'\}$ satisfy the following linear equations and conditions:

$$\left.\begin{aligned} &\Delta\mathbf{v}-\nabla p=0, \quad \nabla.\mathbf{v}=0,\\ &\mathbf{v}=(0,0,U) \quad \text{at} \quad r=\infty,\\ &\Delta\mathbf{v}'-\nabla p'=0, \quad \nabla.\mathbf{v}'=0, \quad \mathbf{v}' \text{ bounded},\end{aligned}\right\} \tag{2.2}$$

$$v_n=v_n'=0, \quad \mathbf{v}_t=\mathbf{v}_t', \quad \boldsymbol{\tau}_t=\alpha\boldsymbol{\tau}_t' \quad \text{at} \quad r=1+f(\theta,\Phi), \tag{2.3}$$

$$\epsilon\tau_n=\epsilon\alpha\tau_n'+a(1/R_1+1/R_2) \quad \text{at} \quad r=1+f(\theta,\Phi), \tag{2.4}$$

where v_n represents the normal velocity component, $\mathbf{v}_t$ the tangential velocity vector, $\boldsymbol{\tau}_t$ the tangential stress vector, τ_n the magnitude of the normal stress, $\alpha=\mu'\mu^{-1}$, R_1 and R_2 are the two principal radii of curvature of the drop surface, and the non-dimensional parameter $\epsilon=\mu U_0 T^{-1}$. Equation (2.4) is Laplace's formula (see Landau & Lifshitz 1959, p. 233) for the equilibrium between the normal stresses across the surface and the tension and curvature of the surface.

We seek the solution $\{\mathbf{v},p\}$ and $\{\mathbf{v}',p'\}$ of (2.2)–(2.4) as expansions valid for small values of ϵ, which are of the form

$$\mathbf{v}=\mathbf{v}_0+\epsilon\mathbf{v}_1+o(\epsilon), \tag{2.5}$$

$$p=p_0+\epsilon p_1+o(\epsilon), \tag{2.6}$$

$$\mathbf{v}'=\mathbf{v}_0'+\epsilon\mathbf{v}_1'+o(\epsilon), \tag{2.7}$$

$$p'=\epsilon^{-1}p_{-1}'+p_0'+\epsilon p_1'+o(\epsilon). \tag{2.8}$$

The parameter α is permitted to be large so long as the deformation of the drop, as a consequence of (2.4), is small. We shall see that the term $\epsilon^{-1}p_{-1}'$ is needed in

order to satisfy condition (2.4). This supposition on p' also ensures the validity of expansion (2.8) for large α. Similarly, we expand $f(\theta, \Phi)$ in the form

$$f(\theta, \Phi) = \epsilon f_1(\theta, \Phi) + o(\epsilon). \tag{2.9}$$

The function f must be $O(\epsilon)$ in order that the drop be spherical when $U_0 \to 0$. We now insert (2.5)–(2.8) into (2.2)–(2.4) and equate coefficients of each power of ϵ in each equation. Thus, at order ϵ^{-1},

$$\nabla p'_{-1} = 0; \tag{2.10}$$

at order ϵ^0,

$$\left.\begin{aligned} &\Delta \mathbf{v}_0 - \nabla p_0 = 0, \quad \nabla . \mathbf{v}_0 = 0, \\ &\mathbf{v}_0 = (0, 0, U) \quad \text{at} \quad r = \infty, \\ &\Delta \mathbf{v}'_0 - \nabla p'_0 = 0, \quad \nabla . v'_0 = 0; \end{aligned}\right\} \tag{2.11}$$

at order ϵ,

$$\left.\begin{aligned} &\Delta \mathbf{v}_1 - \nabla p_1 = 0, \quad \nabla . \mathbf{v}_1 = 0, \\ &\mathbf{v}_1 = 0 \quad \text{at} \quad r = \infty, \\ &\Delta \mathbf{v}'_1 - \nabla p'_1 = 0, \quad \nabla . \mathbf{v}'_1 = 0. \end{aligned}\right\} \tag{2.12}$$

The boundary conditions (2.3)–(2.4) must be examined carefully in order to determine the contributions at the various orders of ϵ.

3. Boundary conditions for the perturbed fields

We express the boundary conditions (2.3) and (2.4) in terms of the spherical co-ordinates (r, θ, Φ). Because $|f| \ll 1$, the terms involving the radii of curvature in (2.4) may be written (Landau & Lifshitz 1959, p. 239) as

$$a/R_1 + a/R_2 = \Delta(r - f), \tag{3.1}$$

where Δ is the Laplacian. It follows that

$$(a/R_1 + a/R_2)_{r=1+f} = 2 - (2 + \Delta_{\theta\Phi})f + O(f^2), \tag{3.2}$$

where

$$\Delta_{\theta\Phi} \equiv \frac{1}{\sin\theta}\frac{\partial}{\partial\theta}\left(\sin\theta\frac{\partial}{\partial\theta}\right) + \frac{1}{\sin^2\theta}\frac{\partial}{\partial\Phi^2}. \tag{3.3}$$

It can be shown (Wohl 1971) that the normal and tangential components of the velocity and stress vectors can be expressed in terms of a co-ordinate system fixed with respect to the local tangent plane of the surface of the deformed drop. Thus, with ϵ_1 and ϵ_2 representing Eulerian angles (see figure 2),

$$v_n = v_r \cos\epsilon_1 \cos\epsilon_2 - v_\theta \sin\epsilon_2 + v_\Phi \sin\epsilon_1 \cos\epsilon_2, \tag{3.4}$$

$$v_{t_1} = v_r \cos\epsilon_1 \sin\epsilon_2 + v_\theta \cos\epsilon_2 + v_\Phi \sin\epsilon_1 \sin\epsilon_2, \tag{3.5}$$

$$v_{t_2} = -v_r \sin\epsilon_1 + v_\Phi \cos\epsilon_1, \tag{3.6}$$

$$\begin{aligned} \tau_{t_1} = {} & (\tau_{rr}\cos^2\epsilon_1 - \tau_{\theta\theta} + \tau_{\Phi\Phi}\sin^2\epsilon_1)\sin\epsilon_2\cos\epsilon_2 + \tau_{r\theta}\cos\epsilon_1(\cos^2\epsilon_2 - \sin^2\epsilon_2) \\ & + \tau_{\theta\Phi}\sin\epsilon_1(\cos^2\epsilon_2 - \sin^2\epsilon_2) + 2\tau_{r\Phi}\sin\epsilon_1\cos\epsilon_1\sin\epsilon_2\cos\epsilon_2, \end{aligned} \tag{3.7}$$

$$\begin{aligned} \tau_{t_2} = {} & (-\tau_{rr} + \tau_{\Phi\Phi})\sin\epsilon_1\cos\epsilon_1\cos\epsilon_2 + \tau_{r\theta}\sin\epsilon_1\sin\epsilon_2 \\ & - \tau_{\theta\Phi}\cos\epsilon_1\sin\epsilon_2 + \tau_{r\Phi}\cos\epsilon_2(\cos^2\epsilon_1 - \sin^2\epsilon_1), \end{aligned} \tag{3.8}$$

$$\begin{aligned} \tau_n = {} & \tau_{rr}\cos^2\epsilon_1\cos^2\epsilon_2 + \tau_{\theta\theta}\sin^2\epsilon_2 + \tau_{\Phi\Phi}\sin^2\epsilon_1\cos^2\epsilon_2 \\ & - 2(\tau_{r\theta}\cos\epsilon_1 + \tau_{\theta\Phi}\sin\epsilon_1)\sin\epsilon_2\cos\epsilon_2 + 2\tau_{r\Phi}\sin\epsilon_1\cos\epsilon_1\cos^2\epsilon_2, \end{aligned} \tag{3.9}$$

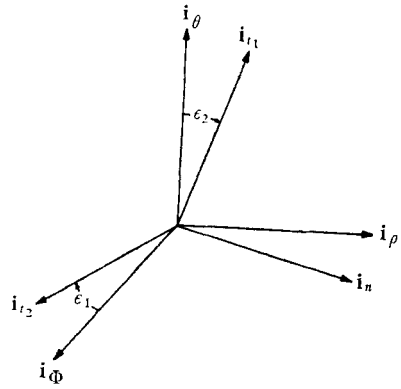

FIGURE 2. Co-ordinate system fixed with respect to the local tangent plane of the surface of the deformed drop. First rotate in the ρ, Φ plane through an angle ϵ_1, then rotate in plane normal to $\mathbf{i}_{t_2}$ through an angle ϵ_2 to obtain this system from that fixed at the centroid of the drop.

where (v_r, v_θ, v_Φ) are velocity components and $(\tau_{rr}, \tau_{r\theta}, \tau_{r\Phi}, \tau_{\theta\theta}, \tau_{\theta\Phi}, \tau_{\Phi\Phi})$ are stress tensor components in spherical co-ordinates. The stress tensor components are expressed in terms of the velocity components as

$$\tau_{rr} = -p + 2(\partial v_r/\partial r), \tag{3.10}$$

$$\tau_{\theta\theta} = -p + 2\left(\frac{1}{r}\frac{\partial v_\theta}{\partial \theta} + \frac{v_r}{r}\right), \tag{3.11}$$

$$\tau_{r\theta} = \frac{1}{r}\frac{\partial v_r}{\partial \theta} + \frac{\partial v_\theta}{\partial r} - \frac{v_\theta}{r}, \tag{3.12}$$

$$\tau_{\Phi\Phi} = -p + 2\left(\frac{1}{r\sin\theta}\frac{\partial v_\Phi}{\partial \Phi} + \frac{v_r}{r} + \frac{v_\theta}{r}\cot\theta\right), \tag{3.13}$$

$$\tau_{r\Phi} = \frac{\partial v_\Phi}{\partial r} + \frac{1}{r\sin\theta}\frac{\partial v_r}{\partial \Phi} - \frac{v_\Phi}{r}, \tag{3.14}$$

$$\tau_{\theta\Phi} = \frac{1}{r\sin\theta}\frac{\partial v_\theta}{\partial \Phi} + \frac{1}{r}\frac{\partial v_\Phi}{\partial \theta} - \frac{v_\Phi}{r}\cot\theta. \tag{3.15}$$

The velocity and stress components for the internal fluid are given by the same expressions with the velocity components and the pressure replaced by their primed counterparts.

The deformation of the sphere is a small quantity and if the surface of the drop is assumed to be sufficiently smooth, it follows that the co-ordinate system of the local tangent plane is obtainable from the spherical co-ordinate system fixed at the centroid of the sphere by means of a small rotation. Therefore, we know that ϵ_1 and ϵ_2 must be small quantities. It is necessary to express them in a quantitative manner in terms of f. To this end, we express the normal vector $\mathbf{i}_n$ as

$$\mathbf{i}_n = \frac{\nabla(r-f)}{|\nabla(r-f)|} = \mathbf{i}_r - \mathbf{i}_\theta\frac{\partial f}{\partial \theta} - \mathbf{i}_\Phi \operatorname{cosec}\theta\frac{\partial f}{\partial \Phi} + O(f^2). \tag{3.16}$$

From (3.4), since ϵ_1 and ϵ_2 are small quantities, we obtain

$$v_n = v_r - \epsilon_2 v_\theta + \epsilon_1 v_\Phi + O(\epsilon_1^2) + O(\epsilon_2^2). \tag{3.17}$$

Comparison of (3.16) and (3.17) shows that we must, for compatibility, require ϵ_1, ϵ_2 and f to be related as follows:

$$\epsilon_1 = -\operatorname{cosec}\theta(\partial f/\partial\Phi), \quad \epsilon_2 = \partial f/\partial\theta. \tag{3.18), (3.19}$$

Substituting (3.18), (3.19) and (2.9) into (3.17), we obtain the expression for v_n in powers of ϵ:

$$v_n = v_r + \epsilon\left\{-\frac{\partial f_1}{\partial\theta} v_\theta - \operatorname{cosec}\theta \frac{\partial f_1}{\partial\Phi} v_\Phi\right\} + o(\epsilon). \tag{3.20}$$

To evaluate v_n on the surface $r = 1 + f = 1 + \epsilon f_1 + \ldots$, we use a Taylor expansion:

$$v_n|_{r=1+f} = v_n|_{r=1} + \epsilon f_1 (\partial v_n/\partial r)_{r=1} + o(\epsilon). \tag{3.21}$$

Substituting (3.20) into (3.21), we obtain

$$v_n|_{r=1+f} = \left\{v_r + \epsilon\left[f_1 \frac{\partial v_r}{\partial r} - \frac{\partial f_1}{\partial\theta} v_\theta - \operatorname{cosec}\theta \frac{\partial f_1}{\partial\Phi} v_\Phi\right]\right\}_{r=1} + o(\epsilon). \tag{3.22}$$

Now, taking account of (2.5), we may obtain the zero- and first-order contributions to $v_n|_{r=1+f}$, namely

$$v_n|_{r=1+f} = \left\{v_{0r} + \epsilon\left[v_{1r} + f_1 \frac{\partial v_{0r}}{\partial r} - \frac{\partial f_1}{\partial\theta} v_{0\theta} - \operatorname{cosec}\theta \frac{\partial f_1}{\partial\Phi} v_{0\Phi}\right]\right\}_{r=1} + o(\epsilon). \tag{3.23}$$

Note that all velocities on the right are now evaluated on the surface of the undeformed sphere $r = 1$ and are expressed as spherical co-ordinate components. It follows in a similar manner that all the other quantities appearing in the boundary conditions (2.3) and (2.4) are expressed to zero and first order in ϵ as follows. At order ϵ^0,

$$v_{0r} = v'_{0r} = 0, \quad v_{0\theta} = v'_{0\theta}, \quad v_{0\Phi} = v'_{0\Phi}, \quad \tau_{0r\theta} = \alpha\tau'_{0r\theta}, \quad \tau_{0r\Phi} = \alpha\tau'_{0r\Phi} \quad \text{at} \quad r = 1, \tag{3.24}$$

$$p'_{-1} = 2/\alpha \quad \text{at} \quad r = 1; \tag{3.25}$$

at order ϵ,

$$\left.\begin{aligned}
&v_{1r} + f_1 \frac{\partial v_{0r}}{\partial r} = [\text{primes}] = \frac{\partial f_1}{\partial\theta} v_{0\theta} + \operatorname{cosec}\theta \frac{\partial f_1}{\partial\Phi} v_{0\Phi},\\
&v_{1\theta} + f_1 (\partial v_{0\theta}/\partial r) = [\text{primes}],\\
&v_{1\Phi} + f_1 (\partial v_{0\Phi}/\partial r) = [\text{primes}],\\
&\tau_{1r\theta} + f_1 \frac{\partial \tau_{0r\theta}}{\partial r} + \frac{\partial f_1}{\partial\theta}(\tau_{0rr} - \tau_{0\theta\theta}) - \operatorname{cosec}\theta \frac{\partial f_1}{\partial\Phi} \tau_{0\theta\Phi} = \alpha\,[\text{primes}],\\
&\tau_{1r\Phi} + f_1 \frac{\partial \tau_{0r\Phi}}{\partial r} - \frac{\partial f_1}{\partial\theta} \tau_{0\theta\Phi} + \operatorname{cosec}\theta \frac{\partial f_1}{\partial\Phi}(\tau_{0rr} - \tau_{0\Phi\Phi}) = \alpha\,[\text{primes}]
\end{aligned}\right\} \text{ at } r = 1, \tag{3.26}$$

$$\tau_{0rr} = \alpha\tau'_{0rr} - (2 + \Delta_{\theta\Phi}) f_1 \quad \text{at} \quad r = 1. \tag{3.27}$$

We note that (3.25) shows why the term $p'_{-1} \neq 0$ is needed in the expansion of p'. It follows that the dimensional internal pressure of a drop in its quiescent spherical shape is $2T/a$. Equations (3.24) involve only the zero-order terms of

the expansion, and (3.27) is an equation for the deformation function f_1 in terms of quantities determined from the zero-order expansion. The function f_1 is determined as a particular solution of (3.27), subject to the conditions that the volume of the drop remains constant,

$$\int_0^{2\pi}\int_0^{\pi}\int_0^{r(\theta,\Phi)} r^2 \sin\theta \, dr \, d\theta \, d\Phi = \tfrac{4}{3}\pi, \tag{3.28}$$

and that the centroid of the drop is chosen to coincide with the origin of the co-ordinate system,

$$\int_0^{2\pi}\int_0^{\pi}\int_0^{r(\theta,\Phi)} \mathbf{r}\, r^2 \sin\theta \, dr \, d\theta \, d\Phi = 0, \tag{3.29}$$

If (2.1) is substituted into (3.28) and (3.29), retaining only terms to first order in f, they become

$$\int_0^{2\pi}\int_0^{\pi} f \sin\theta \, d\theta \, d\Phi = 0. \tag{3.30}$$

$$\int_0^{2\pi}\int_0^{\pi} f \begin{Bmatrix} \sin\theta\cos\Phi \\ \sin\theta\sin\Phi \\ \cos\theta \end{Bmatrix} \sin\theta \, d\theta \, d\Phi = 0. \tag{3.31}$$

To within order-ϵ deformation, we see that the boundary conditions (2.3) and (2.4) expressed on the deformed interface have been transformed to the boundary conditions (3.24), (3.26) and (3.27) expressed on the undeformed sphere surface. The Stokes equations (2.11) and (2.12), subject to the aforementioned boundary conditions and the supplementary conditions (3.30) and (3.31), are now tractable. We shall solve them for the case when **U** is an unbounded parabolic flow using the general method of Lamb (1945, p. 596).

4. Unbounded parabolic flow

We now consider U to be an unbounded parabolic flow defined by

$$U/U_0 = \beta + \delta x + \gamma(x^2+y^2), \tag{4.1}$$

with respect to a co-ordinate system fixed at the centroid of the drop. Here, β, δ and γ are constants and U_0 is a reference velocity. In order to relate this to Poiseuille flow in a tube, let the drop be located at a radial distance b from the tube axis. Suppose that the drop is moving with dimensionless velocity c_0 parallel to this axis, with respect to a co-ordinate system fixed in the tube, and in the same direction as the Poiseuille flow field. If R is the radial component of a cylindrical co-ordinate system measured from the tube axis, then the velocity of the flow with respect to a co-ordinate system fixed at the centroid of the drop (see figure 1) is

$$U/U_0 = 1-(R/R_0)^2 - c_0, \tag{4.2a}$$

where

$$R^2 = (b+ax)^2 + a^2y^2. \tag{4.2b}$$

We shall identify the incident unbounded parabolic flow (4.1) with that given by (4.2a). By comparing these two equations, it follows that

$$\beta \equiv 1-\left(\frac{b}{R_0}\right)^2 - c_0, \quad \delta \equiv -2\frac{ab}{R_0^2}, \quad \gamma \equiv -\left(\frac{a}{R_0}\right)^2. \tag{4.2c}$$

The zero-order velocity field satisfies the boundary condition

$$\mathbf{v}_0 \to \mathbf{k}(U/U_0) \quad \text{as} \quad r \to \infty, \tag{4.3}$$

where $\mathbf{k}$ is the unit vector in the z direction. In this form we see that the order-ϵ^0 velocity and pressure fields are easily obtained by summing the known solutions for a fluid sphere in a uniform stream, linear shear flow and quadratic shear flow, according to the method of Lamb (for details, see Wohl 1971). From these solutions the order-ϵ^0 dimensional hydrodynamic force $\mathbf{F}_0$ on the drop is calculated to be

$$\mathbf{F}_0 = 6\pi\mu a U_0 \left[\frac{\alpha+\frac{2}{3}}{\alpha+1}\beta + \frac{2}{3}\frac{\alpha}{\alpha+1}\gamma\right]\mathbf{k}. \tag{4.4}$$

This is the drag force acting on the undeformed drop. Note that it is independent of the linear shear gradient δ. The original assumption that the drop is in a steady state of motion requires that the net force on the drop be zero, or $\mathbf{F}_0$ plus the body force $\frac{4}{3}\pi a^3 K_0 \mathbf{k}$ equal zero. Therefore we choose c_0, which heretofore has been arbitrary, so that this condition is satisfied, viz.

$$c_0 = 1 - \left(\frac{b}{R_0}\right)^2 - \frac{2\alpha}{3\alpha+2}\left(\frac{a}{R_0}\right)^2 + \tfrac{2}{3}k_0\left(\frac{\alpha+1}{3\alpha+2}\right), \tag{4.5}$$

where k_0 is the non-dimensional body-force parameter given by $k_0 = K_0 a^2/\mu U_0$.

The order-ϵ deformation function f_1 may now be found from (3.27), using (3.10) and the order-ϵ^0 solution. An obvious particular solution of (3.27) which is found also to satisfy the subsidiary conditions (3.30) and (3.31) is

$$f_1 = f_{11} + f_{12},$$

where

$$\left.\begin{aligned} f_{11} &= \tfrac{19}{24}\delta\frac{\alpha+\frac{16}{19}}{\alpha+1}\cos\Phi P_2^1(\cos\theta), \\ f_{12} &= -\tfrac{11}{20}\gamma\frac{\alpha+\frac{10}{11}}{\alpha+1}P_3^0(\cos\theta). \end{aligned}\right\} \tag{4.6}$$

Here P_2^1 and P_3^0 are associated Legendre polynomials (Jahnke & Emde 1945, p. 111). The above result is in agreement with that given by Hetsroni & Haber (1970). It is seen that to order ϵ the deformation of the drop is independent of the uniform flow contribution to U (Saito 1913; Taylor & Acrivos 1964). Also, it is seen that the deformation is independent of the external body force acting on the drop. Therefore f_1 is independent of whether the drop is moving with the flow or held stationary. Four characteristic shapes of the drop in the x, z plane ($\Phi = 0$), based on (2.1) and (4.6) with $\alpha = 0$, are illustrated in figure 3. In figure 3(a), the shape was calculated for $\delta = 0$ and $\gamma = -0{\cdot}04$, for which the shape $f_1 = f_{12}$. This is the shape of the drop for $a/R_0 = 0{\cdot}2$ and $b = 0$, when it is located on the tube axis. In figure 3(d), it was assumed that $\delta = -0{\cdot}2$ and $\gamma = -0{\cdot}04$. This is the shape of the drop for $a/R_0 = 0{\cdot}2$ and $b = \frac{5}{2}a$, when it is located midway between the tube axis and the tube wall. The shape is dominated by the deformation due to linear shear, and $f_1 \approx f_{11}$. In this case, the equation for the shape takes the form $r \approx 1 + \frac{2}{3}\delta P_2^1(\cos\theta)$, which differs from an ellipse by

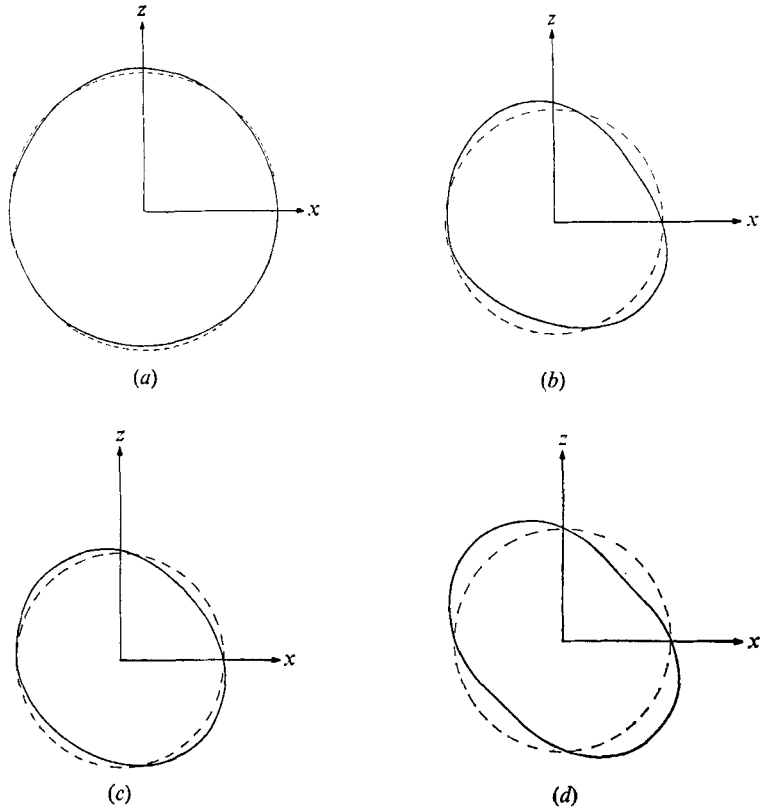

FIGURE 3. Four characteristic shapes of the deformed drop in a Poiseuille flow, calculated according to (4.6). It was assumed that $\alpha = 0$ and (*a*) $a/R_0 = 0{\cdot}2$, $b/R_0 = 0$; (*b*) $a/R_0 = 0{\cdot}4$, $b/R_0 = 0{\cdot}125$; (*c*) $a/R_0 = b/R_0 = 0{\cdot}2$; (*d*) $a/R_0 = 0{\cdot}2$, $b/R_0 = 0{\cdot}5$.

order δ^2. A shape of the drop intermediate between these two extremes is shown in figure 3(*b*), for which $\delta = -0{\cdot}1$ and $\gamma = -0{\cdot}16$. Such a shape is achieved for $a/R_0 = 0{\cdot}4$ with the drop located at $b = \frac{5}{16}a$. A second intermediate shape is shown in figure 3(*c*), for which $\delta = -0{\cdot}08$ and $\gamma = -0{\cdot}04$, which is achieved for $a/R_0 = 0{\cdot}2$ and $b = a$.

To determine the order-ϵ fields $\{\mathbf{v}_1, p_1\}$ and $\{\mathbf{v}_1', p_1'\}$ we must solve Stokes' equations subject to the interface boundary conditions (3.26) at $r = 1$, in addition to having $\mathbf{v}_1$ vanish at infinity. It should be noted that, because a uniform stream produces no deformation of a liquid sphere, the solution for a fluid sphere in a uniform stream is completely determined to any order in ϵ by the order-ϵ^0 solution. We shall show that the order-ϵ solution for unbounded parabolic flow can be expressed as the sum of the known order-ϵ solution for a drop in a linear shear flow, and the known order-ϵ flow produced by a drop in a quadratic shear flow, plus an order-ϵ field needed to satisfy the contribution in the boundary conditions arising from the interaction between the zero-order flow and the first-order deformation of the drop. This interaction does not occur when the flow profiles are considered separately.

To begin we write the order-ϵ^0 parabolic velocity and stress fields explicitly

as the sum of the order-ϵ^0 fields corresponding to a uniform stream ($U = \beta U_0$), linear shear flow ($U = \delta U_0 x$) and quadratic shear flow ($U = \gamma U_0(x^2+y^2)$). Thus, we set

$$\left.\begin{aligned} v_{0r} &= v_{0r}^{(0)} + v_{0r}^{(1)} + v_{0r}^{(2)}, \\ p_0 &= p_0^{(0)} + p_0^{(1)} + p_0^{(2)}, \end{aligned}\right\} \tag{4.7}$$

and similarly for other velocity and stress components, where $v_{0r}^{(i)}$ and $p_0^{(i)}$ correspond to a uniform stream, linear shear flow and quadratic shear flow for $i = 0, 1$ and 2, respectively. For the order-ϵ solution, it is similarly advantageous to separate the contributions arising from the linear shear and quadratic shear flows considered independently. For example, let $v_{1r}^{(1)}$ and $v_{1r}^{(2)}$ represent the aforementioned flow field contributions to v_{1r}. Then define the interaction contributions w_{1r} and $\sigma_{1r\theta}$ by the equations

$$\left.\begin{aligned} v_{1r} &= v_{1r}^{(1)} + v_{1r}^{(2)} + w_{1r}, \\ \tau_{1r\theta} &= \tau_{1r\theta}^{(1)} + \tau_{1r\theta}^{(2)} + \sigma_{1r\theta}. \end{aligned}\right\} \tag{4.8}$$

Substituting (4.8) and analogous expressions for the other first-order velocity and stress components into (3.26) together with (4.6), we find that these boundary conditions can be satisfied in parts as follows:

$$\left.\begin{aligned} &v_{1r}^{(1)} + f_{11}\frac{\partial v_{0r}^{(1)}}{\partial r} = [\text{primes}] = \frac{\partial f_{11}}{\partial \theta} v_{0\theta}^{(1)} + \operatorname{cosec}\theta \frac{\partial f_{11}}{\partial \Phi} v_{0\Phi}^{(1)}, \\ &v_{1\theta}^{(1)} + f_{11}\,\partial v_{0\theta}^{(1)}/\partial r = [\text{primes}], \quad v_{1\Phi}^{(1)} + f_{11}\,\partial v_{0\Phi}^{(1)}/\partial r = [\text{primes}], \\ &\tau_{1r\theta}^{(1)} + f_{11}\frac{\partial \tau_{0r\theta}^{(1)}}{\partial r} + \frac{\partial f_{11}}{\partial \theta}(\tau_{0rr}^{(1)} - \tau_{0\theta\theta}^{(1)}) - \operatorname{cosec}\theta \frac{\partial f_{11}}{\partial \Phi}\tau_{0\theta\Phi}^{(1)} = \alpha[\text{primes}], \\ &\tau_{1r\Phi}^{(1)} + f_{11}\frac{\partial \tau_{0r\Phi}^{(1)}}{\partial r} + \operatorname{cosec}\theta \frac{\partial f_{11}}{\partial \Phi}(\tau_{0rr}^{(1)} - \tau_{0\Phi\Phi}^{(1)}) - \frac{\partial f_{11}}{\partial \theta}\tau_{0\theta\Phi}^{(1)} = \alpha[\text{primes}], \end{aligned}\right\} \tag{4.9}$$

$$\left.\begin{aligned} &v_{1r}^{(2)} + f_{12}\frac{\partial v_{0r}^{(2)}}{\partial r} = [\text{primes}] = \frac{\partial f_{12}}{\partial \theta} v_{0\theta}^{(2)}, \\ &v_{1\theta}^{(2)} + f_{12}\,\partial v_{0\theta}^{(2)}/\partial r = [\text{primes}], \\ &\tau_{1r\theta}^{(2)} + f_{12}\frac{\partial \tau_{0r\theta}^{(2)}}{\partial r} + \frac{\partial f_{12}}{\partial \theta}(\tau_{0rr}^{(2)} - \tau_{0\theta\theta}^{(2)}) = \alpha[\text{primes}], \end{aligned}\right\} \tag{4.10}$$

$$\left.\begin{aligned} &w_{1r} + \frac{\partial}{\partial r}(f_1 v_{0r}^{(0)} + f_{12} v_{0r}^{(1)} + f_{11} v_{0r}^{(2)}) = [\text{primes}] = \frac{\partial f_1}{\partial \theta} v_{0\theta}^{(0)} + \frac{\partial f_{12}}{\partial \theta} v_{0\theta}^{(1)} + \frac{\partial f_{11}}{\partial \theta} v_{0\theta}^{(2)}, \\ &w_{1\theta} + \frac{\partial}{\partial r}(f_1 v_{0\theta}^{(0)} + f_{12} v_{0\theta}^{(1)} + f_{11} v_{0\theta}^{(2)}) = [\text{primes}], \\ &w_{1\Phi} + f_{12}\,\partial v_{0\Phi}^{(1)}/\partial r = [\text{primes}], \\ &\sigma_{1r\theta} + \frac{\partial}{\partial r}(f_1 \tau_{0r\theta}^{(0)} + f_{12}\tau_{0r\theta}^{(1)} + f_{11}\tau_{0r\theta}^{(2)}) + \frac{\partial f_1}{\partial \theta}(\tau_{0rr}^{(0)} - \tau_{0\theta\theta}^{(0)}) + \frac{\partial f_{12}}{\partial \theta}(\tau_{0rr}^{(1)} - \tau_{0\theta\theta}^{(1)}) \\ &\qquad + \frac{\partial f_{11}}{\partial \theta}(\tau_{0rr}^{(2)} - \tau_{0\theta\theta}^{(2)}) = \alpha[\text{primes}], \\ &\sigma_{1r\Phi} + f_{12}\frac{\partial \tau_{0r\Phi}^{(1)}}{\partial r} - \frac{\partial f_{12}}{\partial \theta}\tau_{0\theta\Phi}^{(1)} + \operatorname{cosec}\theta \frac{\partial f_{11}}{\partial \Phi}(\tau_{0rr}^{(0)} + \tau_{0rr}^{(2)}) = \alpha[\text{primes}]. \end{aligned}\right\} \tag{4.11}$$

Equations (4.9) and (4.10) represent the first-order boundary conditions for incident linear shear and quadratic shear flows, respectively, considered independently. The solution for incident linear shear flow was given by Chaffey *et al.* (1965, 1967). The incident quadratic shear flow solution may be found in Wohl (1971). However, the drop does not experience any hydrodynamic force owing to these fields considered independently, and it is therefore not necessary to give them here.

It remains to find a solution to (2.12) which satisfies (4.11) at $r = 1$. Upon inserting the known velocity fields and deformations into (4.11), and applying Lamb's method of solution in a straightforward manner, it is found that the interaction field may be expressed as

$$\left.\begin{aligned}\mathbf{w}_1 &= \tfrac{1}{2}r^2\nabla P_{-2} + 2\mathbf{r}P_{-2} + \tfrac{1}{2}\mathbf{r}P_{-3} - \tfrac{1}{30}r^2\nabla P_{-4} + \tfrac{4}{15}\mathbf{r}P_{-4} - \tfrac{1}{28}r^2\nabla P_{-5} + \tfrac{5}{28}\mathbf{r}P_{-5} \\ &\quad - \tfrac{1}{30}r^2\nabla P_{-6} + \tfrac{2}{15}\mathbf{r}P_{-6} + \nabla(\Phi_{-2} + \Phi_{-3} + \Phi_{-4} + \Phi_{-5} + \Phi_{-6}) \\ &\quad + \nabla\chi_{-3}\times\mathbf{r} + \nabla\chi_{-5}\times\mathbf{r}, \\ p_1 &= \sum_{i=-2}^{-6} P_i,\end{aligned}\right\} \tag{4.12}$$

where P_i, Φ_i and χ_i are solid spherical harmonics defined as follows:

$$\left.\begin{aligned}P_i &= A_i^1 r^i P_{-i-1}^1(\cos\theta)\cos\Phi, \quad \Phi_i = B_i^1 r^i P_{-i-1}^1(\cos\theta)\cos\Phi \\ &\qquad\qquad\qquad\qquad\qquad\qquad \text{for} \quad i = -2, -4, -6, \\ P_i &= A_i^0 r^i P_{-i-1}^0(\cos\theta), \quad \Phi_i = B_i^0 r^i P_{-i-1}^0(\cos\theta) \quad \text{for} \quad i = -3, -5, \\ \chi_{-3} &= C_{-3}^1 r^{-3} P_2^1(\cos\theta)\sin\Phi, \quad \chi_{-5} = C_{-5}^1 r^{-5} P_4^1(\cos\theta)\sin\Phi.\end{aligned}\right\} \tag{4.13}$$

Similarly,

$$\left.\begin{aligned}\mathbf{w}_1' &= \tfrac{1}{5}r^2\nabla P_1 - \tfrac{1}{10}\mathbf{r}P_1 + \tfrac{5}{42}r^2\nabla P_2 - \tfrac{2}{21}\mathbf{r}P_2 + \tfrac{1}{12}r^2\nabla P_3 - \tfrac{1}{12}\mathbf{r}P_3 \\ &\quad + \tfrac{7}{110}r^2\nabla P_4 - \tfrac{4}{55}\mathbf{r}P_4 + \tfrac{2}{39}r^2\nabla P_5 - \tfrac{5}{78}\mathbf{r}P_5 \\ &\quad + \nabla(\Phi_1 + \Phi_2 + \Phi_3 + \Phi_4 + \Phi_5) + \nabla\chi_2\times\mathbf{r} + \nabla\chi_4\times\mathbf{r}, \\ p_1' &= \sum_{i=1}^{5} P_i,\end{aligned}\right\} \tag{4.14}$$

and

$$\left.\begin{aligned}P_i &= A_i^1 r^i P_i^1(\cos\theta)\cos\Phi, \quad \Phi_i = B_i^1 r^i P_i^1(\cos\theta)\cos\Phi \quad \text{for} \quad i = 1, 3, 5, \\ P_i &= A_i^0 r^i P_i^0(\cos\theta), \quad \Phi_i = B_i^0 r^i P_i^0(\cos\theta) \quad \text{for} \quad i = 2, 4, \\ \chi_2 &= C_2^1 r^2 P_2^1(\cos\theta)\sin\Phi, \quad \chi_4 = C_4^1 r^4 P_4^1(\cos\theta)\sin\Phi.\end{aligned}\right\} \tag{4.15}$$

The constant coefficients A_i^j, B_i^j and C_i^j appearing in (4.13) and (4.15) can be determined by applying the boundary conditions (4.11) to the external and internal solutions (4.12) and (4.14) (for details, see Wohl 1971). The resulting linear equations for the 24 coefficients A_i^j, B_i^j and C_i^j divide into seven independent sets, which simplifies their solution.

5. The lift force

To determine the hydrodynamic force on the drop of order ϵ, we need only solve for the coefficient A_{-2}^1. This is so because, for approximately spherical rigid particles whose surface is given by (2.1), the additions to the force and torque

on the particle which are proportional to the deformation are given, respectively, by the expressions (Brenner 1964)

$$\mathbf{F}_1 = -4\pi\mu\epsilon U_0 a \nabla(r^3 P_{-2}), \tag{5.1}$$

$$\mathbf{\Gamma}_1 = -8\pi\mu\epsilon U_0 a^2 \nabla(r^3 \chi_{-2}). \tag{5.2}$$

The force $\mathbf{F}_1$ is additional to the zero-order force $\mathbf{F}_0$ given by equation (4.4). There is no torque on the drop to order ϵ^0, and because $\chi_{-2} = 0$, according to (4.13) there is also no torque on the drop to order ϵ. Upon substituting the expression for P_{-2} from (4.13) into (5.1), we obtain the result

$$\mathbf{F}_1 = -4\pi\mu\epsilon U_0 a A^1_{-2}\mathbf{i}. \tag{5.3}$$

The calculated expression for A^1_{-2} is

$$A^1_{-2} = \beta\delta\frac{57}{160}\frac{(\alpha+\frac{2}{3})}{\alpha}F_{10} - \gamma\delta\tfrac{19}{80}F_{11} - \delta\gamma\tfrac{19}{80}F_{12}, \tag{5.4}$$

where

$$\left.\begin{aligned} F_{10} &\equiv \left[\alpha - \frac{\alpha+1}{3}\left(\frac{R_0}{a}\right)^2 k_0\right]\left(\frac{1}{\alpha+1}\right)^3\left(\frac{1}{\alpha+\frac{2}{3}}\right)(\alpha+\tfrac{16}{19})(\alpha^2-\tfrac{8}{3}\alpha+6), \\ F_{11} &\equiv \left(\frac{1}{\alpha+1}\right)^3(\alpha+\tfrac{16}{19})(\tfrac{9}{8}\alpha^2+\tfrac{41}{672}\alpha-\tfrac{3461}{168}), \\ F_{12} &\equiv -\left(\frac{1}{\alpha+1}\right)^3(\alpha+\tfrac{10}{11})(\tfrac{13541}{3724}\alpha^2-\tfrac{222101}{37240}\alpha+\tfrac{79002}{18620}). \end{aligned}\right\} \tag{5.5}$$

It is observed from (5.4) and (5.5) that the quantities containing F_{10}, F_{11} and F_{12} which contribute to $\mathbf{F}_1$ arise, respectively, from interactions between (*a*) the lag velocity β and the linear shear deformation f_{11}, (*b*) the quadratic shear gradient γ and f_{11}, and (*c*) the linear shear gradient δ and the quadratic shear deformation f_{12}.

Upon insertion of (4.2*c*) and (4.5) into (5.4), we find that

$$\mathbf{F}_1 = \tfrac{19}{10}\pi\mu\epsilon U_0(a/R_0)^4 b(F_{10}+F_{11}+F_{12})\mathbf{i}. \tag{5.6}$$

The expression (5.6) for $\mathbf{F}_1$, which is new, is the main result of this paper. The force $\mathbf{F}_1$ is a lift force, because its direction is orthogonal to the direction of the undisturbed flow at infinity. The magnitude and algebraic sign of $\mathbf{F}_1$ depend on the sum of the coefficients F_{10}, F_{11} and F_{12}, which in turn depend only on the viscosity-ratio parameter α and the dimensionless parameter $k_0 R_0^2/a^2$. The presence of the latter parameter implies that the contribution to $\mathbf{F}_1$ due to the body force is negligible compared with that due to the deformation when $k_0 \ll a^2/R_0^2$ and is dominant when $k_0 \gg a^2/R_0^2$. When $R_0/a \to \infty$, the body-force contribution does not become infinite and in fact vanishes, because of the factor a^4/R_0^4 appearing in the expression (5.6) for $\mathbf{F}_1$. The coefficients and their sum are plotted against α in figure 4 for neutrally buoyant drops, when k_0 is zero. It is seen that F_{10} is always positive, so that the contribution of F_{10} to the lift force is always in the outward radial direction for all values of α. The term F_{11} changes sign from negative to positive as α increases, while F_{12} is always negative. Moreover,

$$F_{10}+F_{11}+F_{12}$$

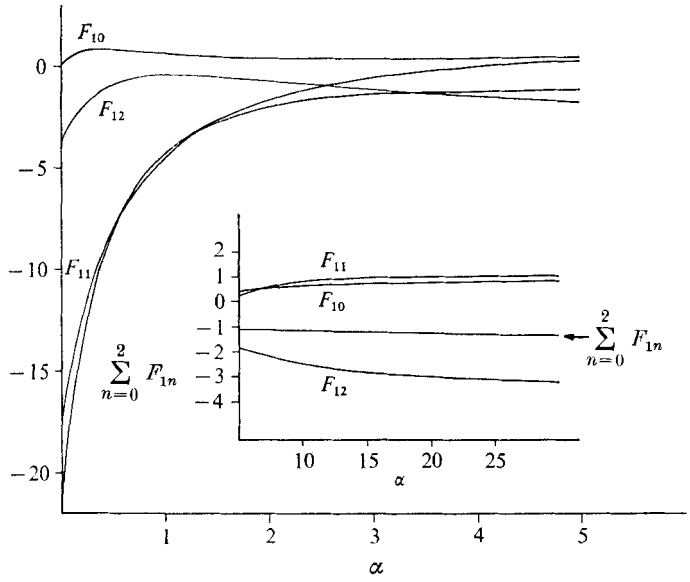

FIGURE 4. Components of the force $\mathbf{F}_{1n}$ defined by (5.5) and (5.6), with the body-force parameter $k_0 = 0$, are shown as a function of the viscosity parameter α. Note that the magnitude of the force $\mathbf{F}_1$, which is proportional to $\sum_{n=0}^{2} F_{1n}$, is always negative. The insert displays the dependence of the components F_{1n} for $\alpha \geqslant 5$. The limit $\alpha \to \infty$ represents the fluid drop becoming rigid.

is always negative, so that the force $\mathbf{F}_1$ on a neutrally buoyant drop always points towards the flow axis. For small α, the coefficient F_{11} makes the largest contribution to the lift force.

Haber & Hetsroni (1971), on the basis of Cox's procedure, have also calculated independently the force $\mathbf{F}_1$. Their result is expressed as a sum of two terms, one proportional to our $\beta\delta$ and another proportional to our $\delta\gamma$. Thus, a direct comparison can be made between our results for F_{10}, and for the sum $F_{11}+F_{12}$. When their expression for F_{10} is compared with ours, it is found that the first four factors on the right-hand side in (5.5) are in agreement, but they obtained the result $\alpha^2+\alpha+\frac{4}{3}$ instead of the last factor. Their expression equivalent to $F_{11}+F_{12}$ is expressed in our notation, to two decimal places, as

$$-1{\cdot}50\alpha^3-0{\cdot}99\alpha^2-1{\cdot}10\alpha-1{\cdot}22.$$

According to (5.5) the sum $F_{11}+F_{12}$ is given to two decimal places by

$$-2{\cdot}51\alpha^3+3{\cdot}67\alpha^2-19{\cdot}37\alpha-21{\cdot}21.$$

Thus we see that the theoretical results are in significant disagreement. The most likely source of this disagreement appears to be algebraic error.

To provide a test of our results, we have examined in §8 the experimental observations of Goldsmith & Mason (1962) of the motion of neutrally buoyant drops in Poiseuille flow, for which $\alpha = 0{\cdot}0002$. The agreement between the experimental observations and the theoretically derived motion of a drop based on the force (5.6) tends to support the present results.

6. The rigid-body limit $\alpha \to \infty$

A casual inspection of (2.4) in conjunction with (3.2) might lead one to infer that the deformation can no longer be small in the limit $\alpha \to \infty$ because the term $\epsilon\alpha\tau'_n$ becomes singular. However, it is important to bear in mind that, for a given incident flow, τ'_n will depend on the parameter α, and therefore a more careful investigation of the limiting process is needed.

To this end, appealing to the primed counterpart of (3.9), together with (2.8), (2.9), (3.18), (3.19) and (3.25), we observe that

$$\tau'_n = \epsilon^{-1}(2/\alpha) + \tau'_{0n} + \epsilon\tau'_{1n} + o(\epsilon), \tag{6.1}$$

where

$$\tau'_{0n} \equiv \tau'_{0rr},$$

$$\tau'_{1n} \equiv \tau'_{1rr} - 2\frac{\partial f_1}{\partial\theta}\tau'_{0r\theta} - 2\operatorname{cosec}\theta\frac{\partial f_1}{\partial\Phi}\tau'_{0r\Phi}, \tag{6.2}$$

with analogous expressions for the internal shear stresses $\boldsymbol{\tau}'_t$ via (3.7) and (3.8). It is tacitly assumed that the order-ϵ^0 and order-ϵ^1 normal and tangential stress contributions are themselves $O(\alpha^{-1})$, if the solution is to be valid when $\alpha = O(\epsilon^{-1})$. However, for a parabolic flow, it is found by direct computation (see Wohl 1971) that τ'_{0n} is $O(\alpha^{-1})$, but $\tau'_{1n} = O(1)$. Furthermore, τ'_{1n} would be $O(\alpha^{-1})$ if the incident linear shear were null. Similarly, all the internal tangential stress components for a parabolic flow to order ϵ^0 and for a quadratic shear to order ϵ are $O(\alpha^{-1})$. But the internal tangential stress components to order ϵ for linear shear are $O(1)$. Thus, the shear stress boundary condition in (2.3) and Laplace's equation (2.4) along with (3.2) cannot be satisfied to order ϵ, when $\alpha = O(\epsilon^{-1})$, for an incident linear shear flow. However, the solution for an incident parabolic flow is valid to order ϵ^0 as $\alpha \to \infty$, and it is also valid to order ϵ as $\alpha \to \infty$ provided that the linear shear portion of the incident parabolic flow field is set equal to zero.

More generally, for flows in which $\alpha\boldsymbol{\tau}'_t$ and $\alpha\epsilon\tau'_n$ remain bounded as $\alpha \to \infty$, it is valid to consider the solutions for the flow and the resultant forces on the drop in the limit $\alpha \to \infty$. The deformed drop then becomes a deformed rigid particle with a given orientation with respect to the incident flow. It is therefore possible to make comparison with known solutions for the Stokes flow past a rigid body, as well as infer some new results. In making this comparison, it is important to realize that we must compare our solution with that for a rigid body of the same shape as the deformed sphere, for which the external torque equals zero. In the remainder of this section, the body force on the drop will be assumed to be absent.

For example, we consider the order-ϵ^0 solution in the special case when the incident flow is just a linear shear, so that $\mathbf{U} = (0, 0, \delta x)$. We find that the flow inside the liquid sphere is given by

$$\mathbf{v}'_0 = \delta\left[\frac{5}{84(\alpha+1)}r^2\nabla(xz) - \frac{1}{\alpha+1}\mathbf{r}(xz) - \frac{3}{4(\alpha+1)}\nabla(xz) - \tfrac{1}{2}(\nabla y)\times\mathbf{r}\right]. \tag{6.3}$$

To this order the shape of the drop remains spherical. In the limit as $\alpha \to \infty$, the internal velocity field becomes

$$\mathbf{v}'_0 = -\tfrac{1}{2}\delta(z, 0, -x). \tag{6.4}$$

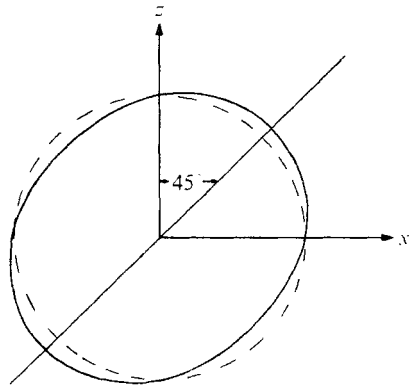

FIGURE 5. The shape of a rigid spheroid according to (6.9), with $\frac{19}{24}\epsilon\delta = \frac{1}{15}$. This is the shape of a fluid sphere deformed by a linear show flow, in the limit as the viscosity of the drop becomes infinite.

The conditions for a fluid motion to be identified as a rigid-body motion are that its shear stresses and divergence vanish, and it is easily verified that $\mathbf{v}_0'$ satisfies these conditions in the limit $\alpha \to \infty$. By considering the curl of $\mathbf{v}_0'$ in this limit, it is seen that

$$\nabla \times \mathbf{v}_0' = (0, -\tfrac{1}{2}\delta, 0), \quad \alpha \to \infty. \tag{6.5}$$

This is recognized to be a rigid-body rotation, equal to $\frac{1}{2}\nabla \times \mathbf{U}$, which is the rotational velocity that a rigid sphere experiences in the incident shear flow $\mathbf{U}$ (Einstein 1906).

As a second example, we consider the solution to order ϵ^0 for the case when the incident flow consists of a uniform flow plus a linear shear flow. In this case, too, the interior flow satisfies the conditions of rigid-body motion in the limit $\alpha \to \infty$. The force on the drop becomes

$$\mathbf{F}_1 = -4\pi\mu\epsilon U_0 a\mathbf{i}\left[\tfrac{3}{10}\delta\left(\frac{1}{\alpha+1}\right)^2\left(\frac{19\alpha+16}{16\alpha+16}\right)(\alpha^2-\tfrac{8}{3}\alpha+6)\right]. \tag{6.6}$$

Furthermore, the drop is deformed by the shear into the spheroid defined by

$$r = 1+\tfrac{19}{24}\epsilon\delta\frac{\alpha+\frac{16}{19}}{\alpha+1}\cos\Phi P_2^1(\cos\theta). \tag{6.7}$$

It is important to recognize here that the order-ϵ deformation is determined by the order-ϵ^0 solution. This deformation is different from that calculated by Taylor (1934), which is that which would be obtained if a small parameter expansion were made in terms of α^{-1}, where $\alpha \gg 1$ and $\epsilon = O(1)$ (Cox 1969). Thus (6.7), which is valid for all α, is complementary to Taylor's result. In the rigid-body limit $\alpha \to \infty$, $\mathbf{F}_1$ becomes

$$\mathbf{F}_1 = -\tfrac{57}{40}\pi\mu\epsilon U_0\delta a\mathbf{i}. \tag{6.8}$$

The equation for the shape of the deformed sphere becomes

$$r = 1+\tfrac{19}{24}\epsilon\delta\cos\Phi P_2^1(\cos\theta), \tag{6.9}$$

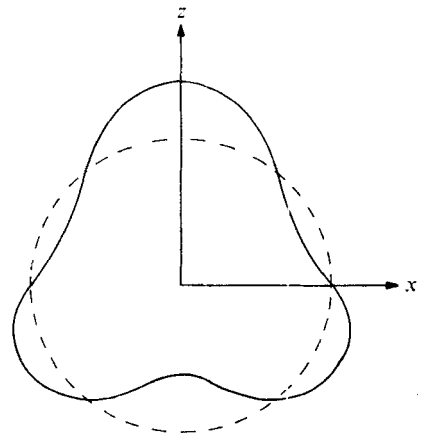

FIGURE 6. The shape of a deformed rigid sphere according to (6.11), with $\frac{11}{20}\epsilon\delta = -0{\cdot}4$. This is the shape of a fluid sphere deformed by a quadratic shear flow, in the limit as the viscosity of the drop becomes infinite.

and is illustrated by figure 5 for $\Phi = 0$ and $\frac{19}{24}\epsilon\delta = \frac{1}{15}$. The force (6.8) is the same as the lateral force (cf. Happel & Brenner 1965, p. 213) produced on a rigid spheroid whose shape is given by (6.9) settling slowly in a viscous fluid. This agreement is to be expected because a linear shear flow produces no force on a drop to order ϵ.

Finally, we note that the order-ϵ solution for uniform plus quadratic shear flow $(0, 0, \beta + \gamma(x^2 + y^2))$, which is valid in the limit $\alpha \to \infty$, predicts that the order-ϵ deformation of the resultant rigid body causes no order-ϵ correction to the order-ϵ^0 drag. Thus from (4.4), with $\alpha \to \infty$, the order-ϵ drag force on the drop is

$$\mathbf{F}_0 = 6\pi\mu a U_0(\beta + \tfrac{2}{3}\gamma)\,\mathbf{k} + O(\alpha^{-1}) + o(\epsilon). \tag{6.10}$$

The shape of the drop, according to (4.6), is

$$r = 1 - \tfrac{11}{20}\epsilon\gamma P_3^0(\cos\theta) + O(\alpha^{-1}), \tag{6.11}$$

and is illustrated in figure 6 for $\frac{11}{20}\epsilon\gamma = -0{\cdot}4$. It is readily verified that the divergence and shear stresses of the interior flow field vanish in the limit $\alpha \to \infty$. Thus, we infer the new result that a rigid spheroid whose shape is given by (6.11) experiences a drag force given by (6.10) when placed in a uniform flow. There is of course no lift force in this case because the incident flow is totally symmetric with respect to the z axis.

7. The trajectory of the drop

We shall now calculate the trajectory of a drop in an unbounded parabolic flow subject to the lift force $\mathbf{F}_1$, where $\mathbf{F}_1$ is given by (5.6). Its radial velocity $d\mathbf{b}/dt$ can be determined by equating the drag force

$$6\pi\mu a \left(\frac{\alpha + \frac{2}{3}}{\alpha + 1}\right) \frac{d\mathbf{b}}{dt}$$

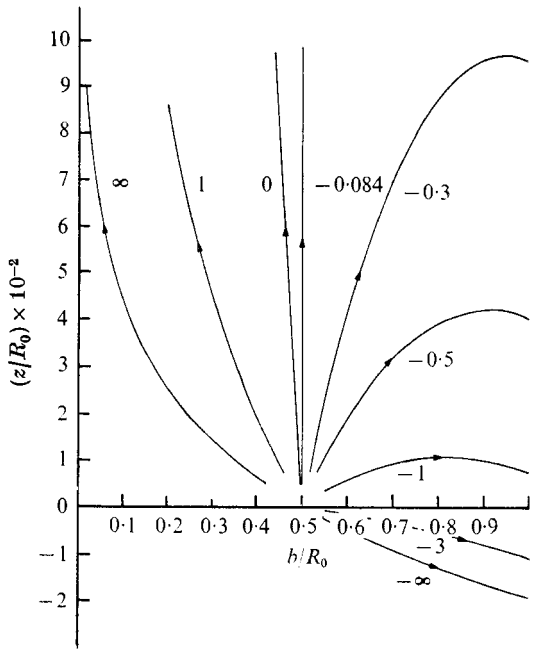

FIGURE 7. The trajectories of a drop in Poiseuille flow and subject to a body force, according to (7.6), with $\alpha = 0$, $\epsilon = 0{\cdot}01$, $a/R_0 = 0{\cdot}1$ and $b/R_0 = 0{\cdot}5$. The labels denote various values of the body-force parameter $k_0 = K_0 a^2/\mu U_0$. The tube axis is represented by the line $b = 0$. The arrowheads indicate the direction of migration as $t \to \infty$. Note that, for $k_0 > -0{\cdot}084$, the drop approaches the tube axis asymptotically, and for $k_0 < -0{\cdot}084$, the drop travels outwards towards the wall.

to $\mathbf{F}_1$. We are justified in applying the drag formula of Hadamard & Rybczynski for a liquid sphere because the deformation makes a negligible contribution to the drag-force coefficient, which is of order ϵ, at most. Consequently, because $\mathbf{F}_1$ is of order ϵ, the correction to $d\mathbf{b}/dt$ would be of order ϵ^2, at most, and can therefore be neglected. Thus, in dimensional co-ordinates,

$$\frac{db}{dt} = -\epsilon \frac{U_0 a^3 b}{R_0^4} F, \tag{7.1}$$

where F is a function of α and $k_0 R_0^2/a^2$ defined by

$$F = -\frac{19}{60}\left(\frac{\alpha+1}{\alpha+\frac{2}{3}}\right) \sum_{n=0}^{2} F_{1n}. \tag{7.2}$$

Integration of (7.1) leads to the result

$$b = b_1 e^{-t/\tau}, \quad \tau = R_0^4/\epsilon U_0 a^3 F, \tag{7.3), (7.4}$$

where b_1 is the initial position of the drop.

To obtain the trajectory of the drop, divide the axial velocity $dz/dt = U_0 c_0$, given by (4.5), by db/dt, given in (7.1). Thus,

$$\frac{dz}{db} = -\frac{R_0^4}{\epsilon a^3 b F}\left[1 + \frac{2}{3}\frac{\alpha+1}{3\alpha+2} k_0 - \frac{2\alpha}{3\alpha+2}\left(\frac{a}{R_0}\right)^2 - \left(\frac{b}{R_0}\right)^2\right]. \tag{7.5}$$

Upon integration we obtain

$$\frac{z}{R_0} = \frac{-1}{\epsilon(a/R_0)^3 F}\left\{\left(1+\frac{2}{3}\frac{\alpha+1}{3\alpha+2}k_0-\frac{2\alpha}{3\alpha+2}\frac{a^2}{R_0^2}\right)\log\left(\frac{b/R_0}{b_1/R_0}\right)-\frac{1}{2}\left[\left(\frac{b}{R_0}\right)^2-\left(\frac{b_1}{R_0}\right)^2\right]\right\}. \tag{7.6}$$

For $b/b_1 \ll 1$, we may drop the last term on the right-hand side, so that (7.6) may be written as

$$b \approx b_1 \exp\left[-z/z_0\right], \tag{7.7}$$

where z_0 is defined by

$$z_0 = R_0^4\left(1+\frac{2}{3}\frac{\alpha+1}{3\alpha+2}k_0-\frac{2\alpha}{3\alpha+2}\frac{a^2}{R_0^2}\right)\Big/\epsilon a^3 F. \tag{7.8}$$

Because we have neglected wall effects in our calculation of $\mathbf{F}_1$, we may reasonably expect the above results to be applicable for tubes and drops for which $a \ll R_0$, so that the wall may be considered to be 'far away' from the drop.

Theoretical curves based on (7.6) are shown in figure 7 for $\alpha = 0$ and the particular choice of the values of the parameters

$$\epsilon = 0{\cdot}01, \quad a/R_0 = 0{\cdot}1 \quad \text{and} \quad b_1/R_0 = 0{\cdot}5,$$

for various values of the dimensionless body-force parameter k_0. These trajectories show that the drop may move inwards or outwards. The direction of migration as $t \to \infty$ for the various values of k_0 can be determined by inspection of (7.1) and (4.5). For $k_0 > -0{\cdot}084$ (to three decimal places), and in particular when there is no body force ($k_0 = 0$), the drop moves in the positive-z direction and approaches the tube axis ($b = 0$) asymptotically. When $k_0 = -0{\cdot}084$, there is no radial migration, and the particle goes to infinity in the positive-z direction along the line $b = b_1$. For $-3 < k_0 < -0{\cdot}084$, the drop moves initially in the positive-z direction and radially outwards. If the flow were actually unbounded, the particle would eventually go to infinity in the negative z-direction, but in an actual tube flow, its trajectory is intercepted by the tube wall. For $k_0 < -3$, the trajectories are always in the negative z direction and radially outwards.

These curves are completely at variance with a similar set of curves presented by Haber & Hetsroni (1971), based on their derived lift force. This disagreement is due not only to the difference in the theoretical value of the magnitude of $\mathbf{F}_1$, but also to an error in sign in equating the lift force to the drag force in the radial direction (their equation (30) *et seq.*).

8. Comparison with experiment

Goldsmith & Mason (1962) have experimentally observed the migration velocity and trajectory of neutrally buoyant liquid drops in a circular tube. We shall compare our theoretical results with their experimental data. They observed the radial position b of the drop as a function of the time, for the para-

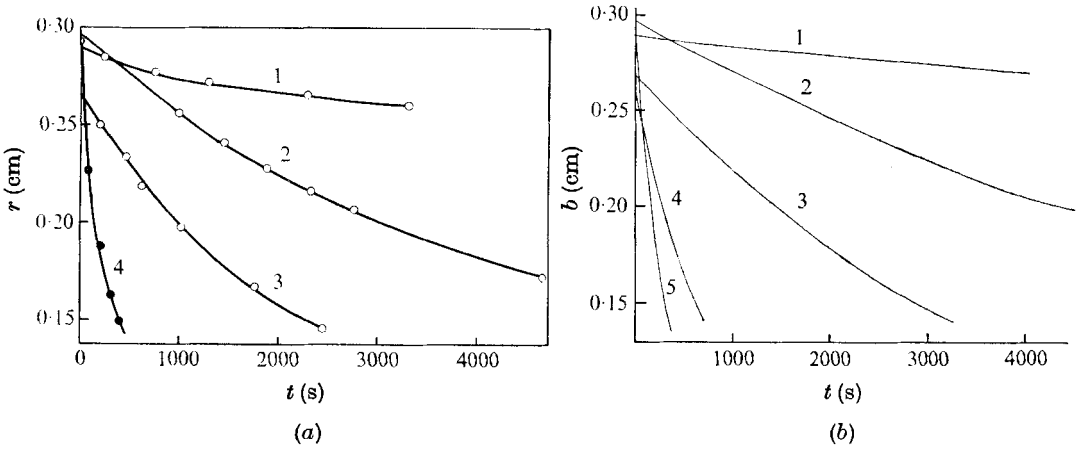

FIGURE 8. (*a*) Radial migration of a neutrally buoyant drop in Poiseuille flow, as observed by Goldsmith & Mason (1962). The curves labelled 1–4 correspond to cases 1–4 of §8. The ordinate labelled r is the same as the radial co-ordinate position b in the text. (*b*) Migration rate of a neutrally buoyant drop in Poiseuille flow, based on (7.3). The values of b_1 (cm) and τ (s) for the various curves are as follows: 1, $b_1 = 0{\cdot}289$, $\tau = 5{\cdot}46 \times 10^4$; 2, $b_1 = 0{\cdot}296$, $\tau = 1{\cdot}08 \times 10^4$; 3, $b_1 = 0{\cdot}268$, $\tau = 4{\cdot}93 \times 10^3$; 4, $b_1 = 0{\cdot}261$, $\tau = 1{\cdot}06 \times 10^3$; 5, $b_1 = 0{\cdot}292$, $\tau = 4{\cdot}29 \times 10^2$. The values of b_1 and τ for curves 1–4 were chosen to be the same as for the experimental curves shown in (*a*).

meter values $\alpha = 0{\cdot}2 \times 10^{-3}$, $\mu = 50{\cdot}3$ P, $R_0 = 0{\cdot}4$ cm and $T = 29{\cdot}0$ dyn cm^{-1}, and for the following cases:

(1) $Q = 0{\cdot}0356$ cm s^{-1}, $a = 0{\cdot}0175$ cm, $b_1 = 0{\cdot}289$ cm;
(2) $Q = 0{\cdot}0356$ cm^3 s^{-1}, $a = 0{\cdot}0300$ cm, $b_1 = 0{\cdot}296$ cm;
(3) $Q = 0{\cdot}0356$ cm^3 s^{-1}, $a = 0{\cdot}0390$ cm, $b_1 = 0{\cdot}268$ cm;
(4) $Q = 0{\cdot}0712$ cm^3 s^{-1}, $a = 0{\cdot}0410$ cm, $b_1 = 0{\cdot}261$ cm;
(5) $Q = 0{\cdot}142$ cm^3 s^{-1}, $a = 0{\cdot}0350$ cm, $b_1 = 0{\cdot}292$ cm;

where Q is the volumetric flow rate in Poiseuille flow; $Q = \pi U_0 R_0^2$. These data are those of system 6 of Goldsmith & Mason. The radial trajectories shown in figure 8(*a*) are taken from Goldsmith & Mason (1962). The trajectories are seen to be directed inwards in all cases. In figure 8(*b*) we have plotted the corresponding theoretical curves, for the same choice of parameter values, based on (7.3) with $k_0 = 0$. A comparison of the two sets of curves in figures 8(*a*) and (*b*) shows that they are in qualitative agreement. Moreover, dependence of the radial velocity on the factor $U_0^2 a^3 b / R_0^4$, predicted by (7.1), has been observed experimentally (Goldsmith & Mason 1962).

A comparison is made in table 1 between the observed and calculated values of $\log(b/b_1)\ (\pi R_0^4)^2/16Q^2a^3t$. According to (7.3) and (7.4), this quantity equals $-\mu F/16T$. In the table the observed values are quoted from Goldsmith & Mason, and are seen to be in general agreement with the theoretical values.

For the same cases, Goldsmith & Mason also observed the radial position of the drop as a function of selected longitudinal positions. These observation points are displayed in figure 9, together with the theoretical trajectories based

System	μ	T	α	$\log (b/b_1)\ (\pi R_0^4)^2/16Q^2a^3t = -\mu F/16T$ Observed	Calculated
6	50·3	25·0	$0{\cdot}2 \times 10^{-3}$	−1·6	−1·3
7	50·3	7·3	$0{\cdot}2 \times 10^{-3}$	−2·6	−4·3
8	50·3	5·0	1·39	−1·6	−1·1

TABLE 1. Values of the quantity $\log (b/b_1)\ (\pi R_0^4)^2/16Q^2a^3t$ observed by Goldsmith & Mason (1962) in their systems 6, 7 and 8, and calculated values based on (7.3), with $k_0 = 0$. Here Q is the volumetric flow rate $\pi U_0 R_0^2$.

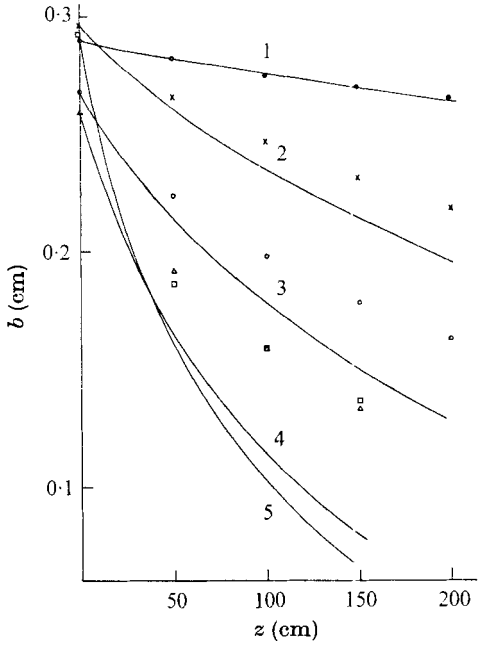

FIGURE 9. Trajectories of a neutrally buoyant drop in Poiseuille flow, based on (7.6) with $k_0 = 0$. The ordinate b measures the distance of the drop from the tube axis, and the abscissa z measures distance down the tube in the flow direction. The labels refer to the five cases observed by Goldsmith & Mason. The observed values of b based on their experimental data, for $z = 50$, 100, 150 and 200 cm, are also indicated for the sake of comparison.

on (7.6). As pointed out in the previous section, neutrally buoyant drops are predicted always to move radially inwards, and the observed trajectories of Goldsmith & Mason are in agreement with this prediction. These observations are also in agreement with other experimental observations (Forgacs, Robertson & Mason 1958; Goldsmith & Mason 1962; Karnis & Mason 1967) on various kinds of neutrally buoyant deformable drops suspended in viscous fluids undergoing Poiseuille flow through circular tubes.

When the theoretical curves in figure 9 are compared quantitatively with the experimental observations, it is seen that there is excellent agreement between

theory and experiment in case 1, for which the radial velocity db/dt is seen in figure 8 (a) to have the smallest value. The discrepancy between theory and experiment is seen to be greater, as the inward radial velocity becomes greater, successively in cases 2–5. The reader should bear in mind that the magnitude of the discrepancy between theory and experiment displayed in figure 9 is exaggerated by the scales of the axes. This discrepancy between theory and experiment remains to be explained. There is a variety of possible theoretical reasons for it, such as effects of second order in ϵ, the effect of the wall and (nonlinear) inertial effects, all of which have been neglected in the present theory.

This work was supported in part by the Office of Naval Research at Cornell University, by NSF Grant GP 20528 at Cornell University Medical College and by the NRC of Canada at Carleton University. We should like to thank Prof. James L. Anderson for an informative discussion pertaining to §6. One of us (P.R.W.) is grateful to Prof. P. Mandl of the Mathematics Department, Carleton University, for support while this paper was being completed.

REFERENCES

BJORKLUND, S. 1965 On the force on a rigid sphere in unbounded Poiseuille flow. Ph.D. thesis, Stevens Institute of Technology, Hoboken, N.J.

BRENNER, H. 1964 *Chem. Engng Sci.* **19**, 519.

CHAFFEY, C. E., BRENNER, H. & MASON, S. G. 1965 *Rheol. Acta*, **4**, 64.

CHAFFEY, C. E., BRENNER, H. & MASON, S. G. 1967 *Rheol. Acta*, **6**, 100.

COX, R. G. 1969 *J. Fluid Mech.* **37**, 601.

COX, R. G. & BRENNER, H. 1968 *Chem. Engng Sci.* **23**, 147.

EINSTEIN, A. 1906 *Ann. Phys.* **19**, 289.

FORGACS, O. L., ROBERTSON, A. A. & MASON, S. G. 1958 *Pulp & Paper Mag. Can.* **59** (5), 117.

FUNG, Y. C. 1966 *Fed. Proc. Am. Soc. Exp. Biol.* **25** (6), 1761.

GOLDSMITH, H. L. & MASON, S. G. 1962 *J. Colloid Sci.* **17**, 448.

HABER, S. & HETSRONI, G. 1971 *J. Fluid Mech.* **49**, 257.

HAPPEL, J. & BRENNER, H. 1965 *Low Reynolds Number Hydrodynamics*. Prentice-Hall.

HETSRONI, G. & HABER, S. 1970 *Rheol. Acta* **9**, 486.

JAHNKE, E. & EMDE, F. 1945 *Tables of Functions*, 4th edn. Dover.

KARNIS, A., GOLDSMITH, H. L. & MASON, S. G. 1963 *Nature*, **200**, 159.

KARNIS, A. & MASON, S. G. 1967 *J. Colloid Sci.* **24**, 164.

LAMB, H. 1945 *Hydrodynamics*, 6th edn. Dover.

LANDAU, L. D. & LIFSHITZ, E. M. 1959 *Fluid Mechanics*. Addison-Wesley.

RUBINOW, S. I. 1964 *Biorheol.* **1**, 117.

RUBINOW, S. I. & KELLER, J. B. 1961 *J. Fluid Mech.* **11**, 447.

SAFFMAN, P. G. 1965 *J. Fluid Mech.* **22**, 385.

SAITO, S. 1913 *Tôhoku Imperial University, Sendai, Japan, Sci. Rep.* no. 2, p. 179.

SEGRE, G. & SILBERBERG, A. 1963 *J. Colloid Sci.* **18**, 312.

TAYLOR, G. I. 1934 *Proc. Roy. Soc.* A **146**, 501.

TAYLOR, T. D. & ACRIVOS, A. 1964 *J. Fluid Mech.* **18**, 466.

WHITMORE, R. L. 1968 *Rheology of the Circulation*. Pergamon.

WOHL, P. R. 1971 The transverse force on a drop in unbounded Poiseuille flow. Ph.D. thesis, Cornell University.